# PredictRoute: A Network Path Prediction Toolkit

*[Paper #126, 16 pages (including references and appendices)]*


## Abstract

Accurate prediction of network paths between arbitrary hosts on the Internet is of vital importance for network operators, cloud providers, and academic researchers. We present PredictRoute, a system that predicts network paths between arbitrary hosts on the Internet using historical knowledge of the data and control plane. In addition to feeding on freely available traceroutes and BGP routing tables PredictRoute optimally explores network paths towards chosen BGP prefixes. PredictRoute's strategy for exploring network paths discovers 4X more autonomous systems (AS) hops than other well-known strategies used in practice today. Using a corpus of traceroutes, PredictRoute trains probabilistic models of routing towards all routed prefixes on the Internet and infers network paths and their likelihood. PredictRoute's AS-path predictions differ from the measured path by at most 1 hop, 75% of the time. A prototype of PredictRoute is live today to facilitate its inclusion in other applications and studies. We additionally demonstrate the utility of PredictRoute in improving real-world applications for circumventing Internet censorship and preserving anonymity online.


## 1 Introduction

Despite its engineered nature, the Internet has evolved into a collection of networks with different–and sometimes conflicting–goals, where understanding its behavior requires empirical study of topology and network paths. This problem is compounded by networks' desire to keep their routing policies and behaviors opaque to outsiders for commercial or security-related reasons. Researchers have worked for over a decade designing tools and techniques for inferring AS level connectivity and paths [20, 21]. However, operators seeking to leverage information about network paths or researchers requiring Internet paths to evaluate new Internet-scale systems are often confronted with limited vantage points for direct measurement and myriad data sets, each offering a different lens on AS level connectivity and paths.

Predicting network paths is crucial for a variety of problems impacting researchers, network operators and content/cloud providers. Researchers often need knowledge of Internet routing to evaluate Internet-scale systems (e.g., refraction routing [29], Tor [8], Secure-BGP [13]). For network operators, network paths can aid in diagnosing the root cause of performance problems like high latency or packet loss. Content providers debugging poor client-side performance require the knowledge of the set of networks participating in delivering client traffic to root-cause bottleneck links. While large cloud providers, like Amazon, Google and Microsoft are known to develop in-house telemetry for global network diagnostics, small companies, ISPs and academics often lack such visibility and data.

Understanding and predicting Internet routes is confounded by several factors. Internet paths are dependant on several deterministic but not public phenomena: route advertisements made via BGP and best path selection algorithms based on private business relationships. Additionally, factors like load balancing via ECMP, intermittent congestion on network links, control plane mis-configurations and BGP hijacks also impact network paths.

Standard diagnostic tools like traceroute provide limited visibility into network paths since the user can only control the destination of a traceroute query, the source being her own network. Tools like reverse traceroute [17] rely on the support of IP options to shed light on the reverse path towards one's network. In addition to requiring the support for IP options from Internet routers, these techniques require active probing from the client (or a set of vantage points distributed on the Internet). Active probing is not only expensive in terms of amount of traffic generated (traceroutes, pings etc.) but also provides limited visibility into the network state.

In this work, we design and develop PredictRoute, which predicts network paths between arbitrary sources and destinations on the Internet by developing probabilistic models of routing from observed network paths. For this purpose, PredictRoute, leverages existing data and control plane measurements, optimizing use of existing data plane measure-

ment platforms, and applying routing models when empirical data is absent. We offer PredictRoute as a service at predictroute.com. In its present form, the PredictRoute REST API allows users to query network paths between sources and destinations (IP address, BGP routed prefix or autonomous system). In addition to providing the predicted paths, PredictRoute provides *confidence* values associated with each network path based on historical information.

PredictRoute complements the approach of existing path-prediction systems [18, 20] by developing efficient algorithms for measuring the routing behavior towards all BGP prefixes on the Internet. When measuring paths towards each BGP prefix, PredictRoute maximizes discovery of the network topology with a constrained measurement budget, both globally and per vantage point. PredictRoute's strategy for exploring network paths discovers 4X more AS-hops than other well known strategies used in practice today.

## 1.1 Key Contributions

The problem of predicting network paths has been well studied, with important work like iPlane [20], iPlane Nano [21], BGPSim [14] and Sibyl [18] tackling different parts of the problem. A detailed discussion of these systems in presented in §9. We define our key contributions in the context of these existing systems:

**Per-destination probabilistic Markov models.** Systems like iPlane and iPlane Nano consume traceroutes to build an atlas of network paths. By combining splices of paths from this atlas, the systems predict a previously un-measured path. Recently, the prediction accuracy of iPlane was found to be low (68% at the AS path level) by Sibyl [18]. Sibyl proposes to improve the low accuracy of splicing based path-prediction of network paths by using supervised learning for choosing between multiple possible paths.

PredictRoute differs from the existing approaches by using the key fact that routing on the Internet is largely destination based [3]. This means, for a given destination prefix, routes from a network are likely to traverse the same path, irrespective where they originated. Therefore, unlike previous path prediction systems, PredictRoute constructs a *destination-specific* probabilistic model for each destination prefix in place of a common atlas for all destination networks. Using observations of network paths over time, PredictRoute not only infers the connectivity between networks but also learns the likelihood of picking different next-hops from a given network.

**Efficient global and per-destination topology discovery.** A related system, Sibyl [18], allows efficient use of measurement budget for answering path queries between sources and destination IP addresses. Instead, PredictRoute focusses on a special case of this problem: efficiently answering *all* queries towards a destination prefix for a fixed measurement budget. PredictRoute's approach for doing measurement selection is within constant factor of optimal in the general case. However, when the routing towards a prefix is destination based, with no violations, we show that PredictRoute's measurement selection is optimal.

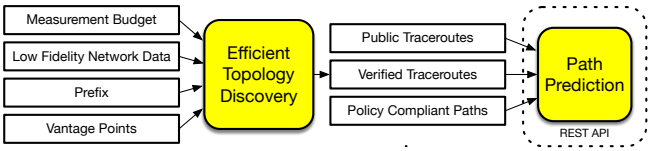


Figure 1: PredictRoute achieves two goals: efficient topology discovery and accurate path prediction.

**Deployment of PredictRoute.** We are releasing the entire codebase of PredictRoute[1]. More importantly, we have deployed PredictRoute in beta version at predictroute.com[2]. We encourage the reviewers to query PredictRoute for paths, either on the website[3] or via the REST API[4]. The REST API can be incorporated programmatically into other systems.

# 2 The PredictRoute System

Figure 1 shows the two major components of PredictRoute along with the input for each. These components are:

1. *Efficient Topology Discovery.* PredictRoute makes efficient use of limited measurement resources to discover the network topology towards an IP prefix. PredictRoute's topology discovery algorithm takes as input a destination BGP prefix $P$, a set of vantage points $V'$ capable of sending traceroutes to $P$, a measurement budget $k$, and information of $P$'s network topology derived from BGP routing tables or older traceroutes (§3.1). This topology discovery algorithm outputs a budget-compliant set of vantage points $S \subset V', |S| \leq k$ from which to measure to reveal as much information about paths towards $P$ as possible (§3.2). In §3, we describe this algorithm and its strong performance guarantees in detail.

2. *Path Prediction.* PredictRoute combines public traceroutes from measurement platforms like RIPE Atlas [24] and those run by its own topology discovery module to learn Markov models of routing towards each BGP routed prefix (§4). PredictRoute infers network paths between source $s$ and destination prefix $P$ from the Markov model (§4). While PredictRoute aims to explore as much

[1] Link/reference omitted to preserve anonymity.

[2] This is an anonymized version of the system hosted in Google's cloud platform for demonstration purposes. Since this is not being hosted on our own infrastructure we use a modestly provisioned cloud instance (a 2 core, 4 GB Google Cloud VM).

[3] *E.g.,* predictroute.com/paths/24.50.160.80/80.252.96.9

[4] *E.g.,* predictroute.com/api/24.50.160.80/80.252.96.9

of the network topology as it can via active measurements, it will still lack a global view due to absence of vantage points in different parts of the Internet. As a result, when a queried path (source $s$ and destination $P$) cannot be inferred from $P$'s empirically-based Markov model, PredictRoute will fall back to an algorithmic simulation of policy-compliant BGP paths [14]. We evaluate how the simulator can be complemented by measured paths to increase prediction accuracy over simulated paths in §5.2.

## 2.1 Design Choices

We now give a brief overview of the design choices made while developing PredictRoute.

**Granularity of predicted network paths.** So far, we have not discussed what constitutes a network path predicted by PredictRoute. In previous research, systems for path prediction have attempted to predict paths at various granularity of intermediate hops. BGPSim [14] returns BGP policy compliant, AS-level paths, whereas iPlane [20], iNano [21], and Sibyl [18] predict PoP-level paths. The granularity of the predicted path can impact its utility for different applications. For instance, AS-level paths can be sufficiently informative for quantifying the threat of eavesdropping ISPs on anonymous communication [23, 26]. However, some ASes can be very large, spanning entire countries (Tier-1 networks like AT&T and Level3), making AS-level path prediction too coarse for diagnostic purposes. Inferring PoPs from router IP addresses is a research problem in its own right PredictRoute avoids introducing the complexity of PoP inference by predicting prefix-level paths. Prefix-level paths have sufficient information to predict AS-level paths by mapping prefixes back to ASes that announce them in BGP to obtain an AS-level path, if desired.

**Markov model for path prediction.** Since paths on the Internet are an outcome of several un-observable and uncertain phenomenon, it is natural to model their behavior using empirically derived probabilistic models. PredictRoute builds a Markov chain, one for each routed prefix $P$, using traceroutes that share a destination $P$. With the routed prefix as the *end state*, other routed prefixes on the Internet act as potential *start states* of the Markov chain, the problem of network path prediction is to find the most likely sequence of states from a given start state to the end state. PredictRoute additionally offers users the ability to predict paths based only on traceroutes performed during a specified window of time.

**Granularity of destinations.** While existing simulation approaches focus on paths towards destination ASes [14], we observed many violations of destination-based routing when considering destinations at the AS-level, since large ASes announce several prefixes, each getting routed to differently. This led us to our decision to construct Markov chains on a per-prefix basis. While BGP atoms [2] may have reduced the storage requirements of the per-prefix Markov chains, previous research [22] shows that over 70% of BGP atoms consist of only one IP prefix, limiting the potential reduction.

# 3 Efficient Topology Discovery

In this section, we discuss the problem of discovering the set of paths towards a destination prefix $P$. PredictRoute's measurement algorithm aims to maximize the amount of the Internet topology discovered when measuring paths towards $P$. It begins by using existing but imperfect data sources to construct a graph representation of the network topology. Existing data sources can be BGP paths, which are known to differ from data plane measurements or stale traceroutes which may not match the current network state (§3.1).

We frame the challenge of maximizing per-prefix topology discovery for a given measurement budget as an optimization problem, which we show is equivalent to a special case of the MAX-COVER$_k$ (§3.2) problem when routing is destination-based and present a greedy algorithm (§3.3) that optimally solves this topology discovery problem. In the case where networks violate destination-based routing, we can still guarantee a constant-factor approximation of the problem using a relaxation of the MAX-COVER$_k$ problem (§E).

## 3.1 Existing Data Sources

We build an initial network topology of paths towards prefix $P$ using the BGPSim [14] path simulator. BGPSim computes BGP policy compliant paths between any pair of ASes. So, for any prefix $P$, we find the policy compliant paths from all ASes on the Internet to the AS announcing prefix $P$. We note that this implies that the BGPSim derived topologies of all prefixes in the same AS are the same. The result of this computation is a tree of ASes rooted at the origin AS for $P$. If pre-existing traceroute data is used to augment the graph produced by BGPSim, the graph might have cycles when traceroutes include paths that existed at distinct time periods or when data- and control-plane paths do not agree. These cycles may also exist as a result of violations of destination-based routing [3]. We discuss cycles we observe and their implications on our results in Section 5.1.

## 3.2 Maximizing Topology Discovery

We define the destination-based DAG of a prefix $P$ as $G = (V, E)$, where $V$ consists of $P$ and all ASes. Edge $e \in E$ represents an observed connection between two ASes. We consider the prefix as the root of this graph as opposed to the AS that announced it to account for per-prefix routing policies [3]. $V' \subset V$ is the set of ASes that have vantage points.

In practice, for a given prefix $P$, we do not know $G$. By executing traceroutes from a subset $S$ of $V'$, we obtain a *partial*

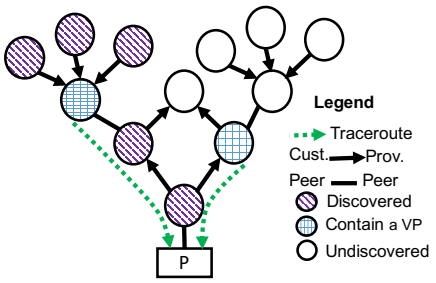


Figure 2: Example of a prefix-based DAG.

*observation* of $G$ denoted by $\hat{G} = (\hat{V}, \hat{E})$. $\hat{V}$ is composed of AS hops observed in traceroutes from ASes in $V'$ towards $P$. Edges in $\hat{E}$ consist of AS edges inferred from traceroutes[5]. Let the coverage of a set of measurements from $S \subset V'$ be:

$$\text{Cov}(S) = |\hat{E}| \tag{1}$$

Figure 2 illustrates one such prefix-based graph. The blue/hashed nodes indicate networks containing vantage points (*e.g.,* RIPE Atlas probes) and the purple/striped nodes indicate nodes that are discovered via traceroutes and single-homed customers of networks containing vantage points. Here $\hat{V}$ is the set of shaded nodes and $\hat{E}$ are the edges that connect them. White nodes represent nodes that we cannot discover via measurements towards $P$.

This leads us to the following problem definition for exploring the largest portion of the AS topology ($G$) with a fixed measurement budget of $k$ traceroutes:

**Problem 1** (PREFIX-COVER$_k$)**.** *Find $S \subset V'$, where $|S| \leq k$, that maximizes* Cov$(S)$.

The PREFIX-COVER$_k$ problem is reducible to the MAX-COVER$_k$ problem in which the input is a number $k$ and a collection $\mathcal{A} = \{A_1, A_2, \ldots\}$ of sets and the goal is to select a subset $\mathcal{A}' \subset \mathcal{A}$ of $k$ sets that maximizes $|\cup_{A \in \mathcal{A}'} A|$. The reduction is immediate since each vantage point measurement can be thought of as a set $A_i$, and our goal is to maximize the coverage of edges by choosing $k$ of these sets. MAX-COVER$_k$ is unfortunately NP-Hard. A well-known greedy algorithm provides the best possible approximation with a factor of $(1-1/e) \approx 0.63$ of the optimal solution [9]. However, since PREFIX-COVER$_k$ is a special case of MAX-COVER$_k$, where the $G$ is largely expected to be a tree, we find that it can be solved exactly which we discuss in the next section.

## 3.3 Optimality for Destination-based Routing

We now discuss how a greedy algorithm to select vantage points (Algorithm 1) yields the optimal solution to PREFIX-COVER$_k$ when the graph $G$ is a tree.

[5]Infering AS-level connectivity from traceroutes is known to be a thorny issue [7]. We discuss details of our approach to this problem in Appendix A

**Algorithm 1:** Greedy Vantage Point Selection

**Input:** Graph $G = (V, E)$ with vantage points $V'$.
$S \leftarrow \emptyset$
**for** $i = 1$ *to* $k$ **do**
  $S \leftarrow S + \text{argmax}_{s \in V'} \text{Cov}(S + s)$
**end**
**return** $S$

**Theorem 1.** *Algorithm 1 solves* PREFIX-COVER$_k$ *exactly when $G$ is a tree, i.e., when there are no violations of destination-based routing.*

*Proof.* Let $S = \{s_1, s_2, \ldots, s_k\}$ denote the subset of vantage points returned by the greedy algorithm on $G$, where $s_1$ denotes the first vantage point chosen, $s_2$, denotes the second, and so on. Recall that Cov$(S)$ denotes the coverage on $G$ of the measurements run from $S$, and let $\mathcal{C}(S)$ denote the corresponding set of edges that are discovered. For the sake of contradiction assume that for some $i < k$, there is an optimal solution $T$ such that $s_1, \ldots, s_{i-1} \in T$ but no optimal solution contains $s_1, \ldots, s_i$. Let

$$T = \{s_1, s_2, \ldots, s_{i-1}, t_i, t_{i+1}, \ldots t_k\}$$

where $s_i \neq t_j$ for all $j \geq i$. In other words, we assume that for some $i$, the first $i-1$ vantage points in $S$ are also in $T$, but that $s_i$ does not appear in $T$. For any set of vantage points $A$, define

$$\mathcal{C}'(A) = \mathcal{C}(A) \setminus \mathcal{C}(s_1, s_2, \ldots, s_{i-1})$$

and $\text{Cov}'(A) = |\mathcal{C}'(A)|$.

For any $j \geq i$, since $s_i$ was chosen by the greedy algorithm before $t_j$ we can infer that

$$\text{Cov}'(s_i) \geq \text{Cov}'(t_j) \ .$$

Let $j' \geq i$ be chosen to maximize $|\mathcal{C}'(s_i) \cap \mathcal{C}'(t_{j'})|$ and define $T' = (T \cup \{s_i\}) \setminus \{t_{j'}\}$. Observe that

$$\text{Cov}'(T') \geq \text{Cov}'(T) + \text{Cov}'(s_i) - \text{Cov}'(t_{j'})$$

Since $\text{Cov}'(s_i) \geq \text{Cov}'(t_{j'})$, we deduce that $\text{Cov}(T') \geq \text{Cov}(T)$ and so $T'$ is also optimal. But $s_1, \ldots, s_i \in T'$ which is a contradiction to the assumption that no optimal solution contains $\{s_1, \ldots, s_i\}$. □

## 3.4 Violations of Destination Based Routing

**Prior-hop violations of destination-based routing.** When merging multiple traceroute-derived AS paths we observe cases that violate destination-based routing. Figure 3 shows one such example. Here, we observe AS 3356 (Level 3) selecting different next-hop ASes towards the same prefix, depending on the prior hop in the path[6]. In this case, it appears

[6]To exclude the effect of churn in network paths, these traceroutes were run only a few minutes apart.

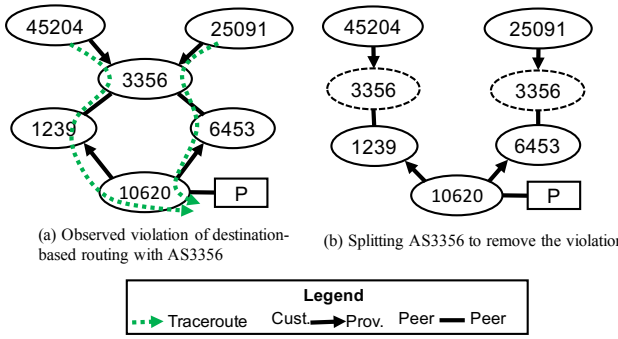


(a) Observed violation of destination-based routing with AS3356

(b) Splitting AS3356 to remove the violation

Figure 3: Example of violation of destination-based routing. Depending on the prior hop AS 3356 (Level 3) selects a different next-hop towards the destination. Splitting this node produces a tree-structured prefix DAG.

Level 3's routing decision is impacted by the prior AS hop, thus we can "split" the node into two nodes, each of which represents Level 3's routing behavior for each of the prior hops. The resulting graph is now a tree.

In general, we can split AS nodes that violate destination-based routing based on their prior AS hop by creating a copy of the node for each prior hop, and adding to each copied node all outgoing edges associated with that prior hop.

The result of this process is a tree with the same number of edges as the original graph. We can run our greedy algorithm on this tree and optimize discovered coverage as before.

**Other violations of destination-based routing.** Not all violations of destination-based routing are based on the prior AS hop. In these cases, it is often difficult to determine exactly what rule underlies the routing behavior and we simply treat this behavior as a random process. In Appendix E, we discuss an extension to the algorithm discussed in Section 3.3 which attempts to maximize coverage subject to this random routing behavior. We present two algorithms which trade off between coverage quality and parallelizability (i.e., whether the measurements must be decided ahead of time or whether each measurement depends on the outcome of previous measurements). We prove that the serial algorithm achieves an approximation factor of at least $1-1/e$, while the parallelizable algorithm achieves an approximation factor of at least $(1-1/e)^2$.

## 3.5 Evaluating the Greedy Algorithm

We now evaluate the performance of our greedy algorithm in discovering paths towards a given prefix $P$. The results of the measurements dictated by the algorithm is a directed acyclic graph (DAG) rooted at $P$. We evaluate the performance of our algorithm and others based on the number of nodes observed in the per-prefix DAGs. We compare our greedy algorithm to random vantage point selection and a geodistributed algorithm that selects probes from as many countries as possible (*i.e.,* it will not pick a second probe from a given country until all other countries have been selected).

We first consider how well the greedy algorithm performs relative to random or geodistributed measurement strategies. Figure 4 shows the number of ASes discovered in DAGs for destination prefixes for different numbers of measurements. The solid line represents the median and dashed lines containing the shaded area show the $5^{th}$ and $95^{th}$ percentiles. We perform this evaluation using algorithmic simulation [14] but in Appendix D we show that simulated paths and coverage results match well with actual measurement values.

**The greedy strategy is able to cover more ASes for a given measurement budget.** We find that for the same number of measurements ($k = 500$), our greedy strategy is able to cover 4 times more ASes than both random and geo-distributed strategies. The random strategy observes a linear increase in the number of ASes covered for a given probing budget, whereas the greedy strategy selects probes that will increase coverage the most early on. After a certain point the benefit of adding more measurements shows decreasing returns.

**Results are robust across prefix types.** We find that our results are robust across different prefix types (Appendix, Figure 14).

**Results are robust across measurement platforms.** We consider the coverage predicted for different measurement budgets using our greedy algorithm across different measurement platforms in Figure 4. We find that, across the three measurement platforms the greedy probe selection algorithm maximizes the number of ASes covered for a given measurement budget. Across the three platforms, random and geodistributed perform similarly, with the exception of the CAIDA Ark platform, where forcing the system to measure from all countries actually results in lower coverage than would be seen by even the random strategy.

**Benefit of including single homed stub ASes.** We add single homed stub customers of vantage point ASes to the discovered topology. Since these stubs are single homed, knowing the path from their provider to the destination prefix ensures knowledge of the path from the stub as well. We evaluate the coverage of the greedy algorithm in the absence of gains from single homed ASes. Figure 5 shows that our algorithm clearly performs better than other measurement strategies even when excluding coverage gains of single-homed stubs.

**Scaling PredictRoute.** We now evaluate the load imposed on RIPE Atlas probes if a maximum of 500 (k = 500) PredictRoute proposed optimized measurements are run towards all destination ASes on the Internet. Figure 6 shows the distribution of number of traceroutes per probe, if the per-destination AS measurement budget is capped at 500 (we run a maximum 500 traceroutes towards any destination AS). We see that 75% of RIPE Atlas probes would need to execute less than 2000 traceroutes.

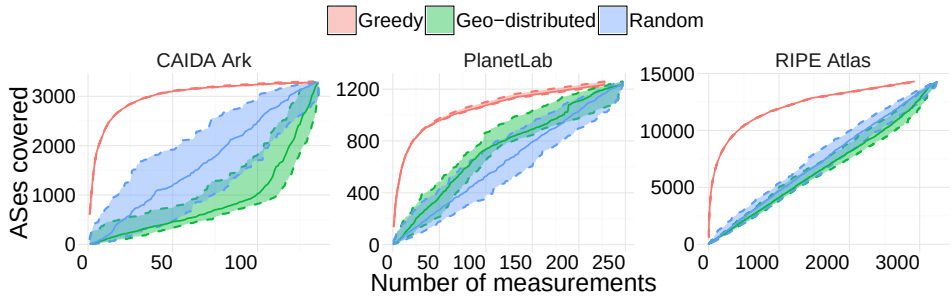


Figure 4: The number of ASes discovered in the DAGs for different measurement budgets and different measurement strategies, across three measurement platforms: (1) CAIDA Ark (2) PlanetLab, and (3) RIPE Atlas. Results shown for content-heavy prefixes

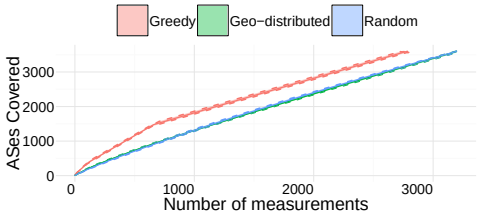


Figure 5: ASes covered in the graphs of high content prefixes when excluding gains from single-homed stub ASNs.

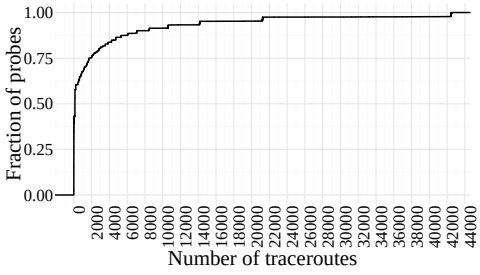


Figure 6: Distribution of the number of traceroutes that each RIPE probe would need to run if the greedy algorithm was scaled to all destination ASes on the Internet.

# 4 Path Prediction

In this section, we outline how PredictRoute uses empirical data to predict paths. Section 4.1 explains how PredictRoute builds destination specific graphs and auxiliary tables to capture the routing behavior towards a prefix. Section 4.2 details how PredictRoute uses this information to define Markov chains for predicting paths between source and destination hosts on the Internet. Section 4.3 explains how simulations are used to fill in gaps in the Markov chains derived from traceroutes, enabling PredictRoute to predict paths for all queries to a measured prefix.

## 4.1 Constructing per-prefix DAGs

We gather a set of traceroutes publicly available on measurement platforms and those run in the topology discovery stage of PredictRoute. We aggregate traceroute hops into BGP routed prefixes to make up the nodes in the DAGs. The process of converting IP paths to prefix-level (or AS-level) paths is involved and requires handling of complex corner cases. We have summarized our procedure in Appendix A.

Let $\mathcal{P}$ be the set of discovered paths prefix-level paths derived from traceoutes. The process of constructing trusted per-destination graphs has two main components, generating the graph itself and computing the auxiliary "transition tables" that will be used to predict the sequence of edges that a path will take in the graph towards the destination prefix.

1. **DAG Construction:** Take the union of all edges in the paths in $\mathcal{P}$ to form the directed acyclic graph $\mathcal{D} = (V, E)$.

2. **Basic Transition Table:** For each edge $e \in E$, let $c_e$ be the count of the number of paths including $e$.

**Temporal transition tables and compression.** We will be interested in predicting paths both based on the entirety of the observed data and based on data observed during a window of time. To support the latter, we need to augment our basic transition tables with an additional dimension. Let $t \in \{1, 2, \ldots, T\}$ index the relevant time period (*e.g.,* the last month or year) at the required resolution (*e.g.,* hours or days). Let $\mathcal{P}_t$ be the set of discovered paths at time $t$ and let $c_e^t$ be the number of paths in $\cup_{t' \geq t} \mathcal{P}_{t'}$ that includes $e$. By defining $c_e^t$ in this way, note that $c_e^{t_2} - c_e^{t_1}$ is the number of paths in $\cup_{t_1 \leq t' < t_2} \mathcal{P}_{t'}$ that include $e$ and this can be computed in $O(1)$ time rather than in $O(t_2 - t_1)$ time.

Unfortunately, storing $c_e^1, c_e^2, \ldots, e_e^T$ rather than just $c_e$ increases the space to store the tables by a factor $T$ and this may be significant. To ameliorate this situation, note that $c_e^t$ is monotonically decreasing with $t$ and hence it suffices to only store values for $t$ where $c_e^t \neq c_e^{t-1}$ as the other values can be inferred from this information. By trading-off a small

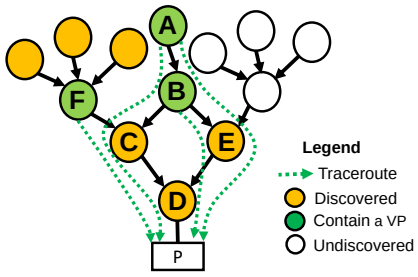


Figure 7: A DAG constructed from trusted traceroutes. Vantage point $A$ sends two traceroutes which follow paths $ABCD$ and $ABED$. $B$ sends one traceroute with path $BED$ and $F$ sends one traceroute with path $FCD$.

amount of accuracy we can further reduce the space as follows. Suppose we are willing to tolerate a $1+\varepsilon$ factor error in the values of $c_e^t$. Then, round each $c_e^t$ to the nearest power of $1+\varepsilon$ and let $\tilde{c}_e^t$ be the resulting value. Then only storing $\tilde{c}_e^t$ for values of $t$ where $\tilde{c}_e^t \neq \tilde{c}_e^{t-1}$ allows every $c_e^t$ to be estimated up to a factor $1+\varepsilon$ whilst only storing at most $1+\log_{1+\varepsilon}(c_e^1)$ different values.

## 4.2 Path Prediction via Markov Chains

**Learning transition probabilities.** The graph for a given prefix $P$ derived from traceroutes towards $P$ defines the structure of the Markov chain PredictRoute uses for modeling the routing behavior towards the prefix. PredictRoute computes the transition probabilities of each Markov chain using Maximum Likelihood Estimation (MLE), given the traceroute counts stored in edge transition tables. With each edge $e \in E$ we assign a probability $p_e = c_e / \sum_{f \in N_u} c_f$ where $N_u$ is the set of outgoing edges of $u$. If the user wishes to only train using traceroutes in a time window $\{t_1, t_1+1, \ldots, t_2-1\}$ we set $p_e = (c_e^{t_1} - c_e^{t_2}) / \sum_{f \in N_u} (c_f^{t_1} - c_f^{t_2})$

Once the Markov models are trained, PredictRoute obtains one Markov chain per destination prefix, where the states of the Markov chain represent BGP prefixes and the end state is the destination prefix $P$. Edges between the states are evidence of traffic towards $P$ traversing them and the edge transition probabilities define the likelihood of traffic traversing that edge. An example Markov chain is shown in Figure 7. In this chain $A$, $B$, $C$, and $D$ are prefixes. We want to calculate the probability that a packet sent from source prefix $A$ to destination prefix $D$ follows the path $A \to B \to C \to D$.

**Defining path probabilities.** PredictRoute assumes probabilistic routing obeys a first-order Markov property. In other words, the probability of a packet choosing a next hop towards destination $P$ only depends on the current hop. This dependence on current hops rather than all prior hops is inspired by the prevalence of next-hop routing on the Internet [15]. For the example in Figure 7, this first-order Markov assumption allows us to express the probability of the specified path as

$$\Pr(A,B,C,D) = \Pr(A) \cdot \Pr(B|A) \cdot \Pr(C|B) \cdot \Pr(D|C)$$

Since we have specified that the path begins at $A$, $\Pr(A) = 1$. In this case, $\Pr(B|A) = 1$ since all traceroutes originating from $A$ go to $B$. $\Pr(C|B) = 1/3$ since there are 3 traceroutes that go through $B$, and one of them has next hop $C$. $\Pr(D|C) = 1$ since both of the traceroutes that go through $C$ have a next hop of $D$. So $\Pr(A,B,C,D) = 1/3$.

**Inferring most likely sequence of states.** A naive way of predicting paths from prefix Markov chains would enumerate all paths from the source node $S$ to the destination prefix $D$ and return the one with the highest probability. However, a graph can have an exponential number of paths between the source and the destination, making this approach prohibitively expensive. A more efficient approach is as follows: for each edge $e = (u,v)$ define the length $\ell_e = -\log(p_e)$. This weight is always nonnegative and will be high if $p_e = \Pr(v|u)$ is low and vice versa. Furthermore, the probability of a path is inversely proportion to its length. We then find $r$ shortest paths using Yen's algorithm [31] where the length of $e$ is set to $\ell_e$; these correspond to the $r$ paths with the highest probability. We set $r = 5$ in PredictRoute's current implementation. PredictRoute returns a ranked list of these paths and their respective probabilities in response to a path query.

## 4.3 Splicing Empirical and Simulated Paths

If PredictRoute is faced with a query between a source AS and a destination prefix such that the source AS is not a state in the Markov chain of the destination prefix, it cannot predict the path using the chain alone. In such situations we query BGPSim for a policy compliant path from the source AS to the destination prefix. We keep each hop of this path, starting from the source ASN, until we reach an ASN that is present in the Markov chain for destination prefix. We predict the path between the ASN at the splice point and the destination prefix using methods described in the previous subsection. In this manner, PredictRoute can still return probability-ranked paths for such a query by considering the BGPSim splice of the path as fixed (with transition probabilities of 1).

# 5 PredictRoute System Evaluation

In this section we discuss how we learned the PredictRoute per-prefix Markov chains and their edge transition probabilities. We then characterize the Markov chains and demonstrate the accuracy of the paths they predict. We note that

## 5.1 Implementation

**Training.** For training PredictRoute per-prefix DAGs, we acquire all public traceroutes available on RIPE Atlas from

December 25, 2018 until March 4, 2019. These traces consist of those that are run by the developers of the platform and those that users run for their own experiments. The scale of these measurements is large, with nearly 2.5-3 million traceroutes being run on the platform every hour. In this manner, we use 4.5 billion public traceroutes to learn the routing behavior towards 545,168 Markov chains, one for each routed prefix on the Internet. In Appendix A we describe the procedure for converting traceroutes to prefix-level and AS-level paths. The edges of the Markov chains store the first order transition probability, derived by Maximum Likelihood Estimation on the set of traceroutes.

We construct graphs for prefixes at two different granularities. In the first kind, all nodes in the graph, including the destination prefix are BGP routed prefixes. In the second kind, all nodes in the graph except the destination prefix represent ASes. Our goal with these two kinds of graphs is to aggregate information at different levels, allowing the users to pick which works for their application.

In the worst case, a prefix gran can have as many nodes as the number of prefixes on the Internet ($\approx 500,000$). This size is fairly large compared to the AS-level graphs which in the worst case have as many nodes as the ASes on the Internet($\approx 60,000$). However some applications require fine-grained paths where intermediate hops are prefixes (§7) while others only need AS-level paths (§7).

**Characteristics of PredictRoute's destination prefix graphs.** Since we train the PredictRoute graphs on public traceroutes on RIPE Atlas, here we understand the impact of duration of data collection on the size of graphs learned. Figure 8(a) shows the distribution of graph sizes as the duration of data collection increases from 1 week to 8 weeks. Each hour of results adds 3 million traces to PredictRoute's processing pipeline, so we stop at 9 weeks of data for the evaluation of prefix graphs. We note that, in practice prefix graphs have $< 15,000$ nodes, much lesser than the theoretical worst case. This can be explained by the shrinking of Internet paths due to the flattening of the Internet topology [12].

Interestingly, we observe some cycles in our learned prefix graphs. These cycles motivate the inference methodology we use for predicting paths from the graphs (discussed at the end of this section). While several cycles were found within ASes, we found a few that crossed the boundaries of ASes. Cyclical structure across AS boundaries suggest routing instability or delayed BGP convergence. we analyze the age of these cycles as the common duration of time when all edges of the cycles were observed in traceroutes. Figure 8(b) shows the distribution of inter-AS cycles age in hours. We note that these cycles are often short lived and rare. We provide insights into one such inter-AS cycle and think PredictRoute's graphs provide a new lens to study routing instabilities on the Internet (§8).

**Inference.** The problem of predicting the network path from a source node to the destination prefix in the Markov chain, is that of finding the likeliest sequence of states from the source to the destination state. Since enumeration of paths in the cyclical Markov chain can be expensive, we adapt Yen's $r$-shortest paths algorithm to our problem for finding $r$ most likely paths between the source and destination. The likelihood of a path is calculated with the first order Markov assumption as described in §4.2. Note that Yen's algorithm returns only loopless paths, ensuring that even if a destination prefix graph contains cycles PredictRoute will never predict cyclical paths.

## 5.2 Accuracy of Predicted Paths

To evaluate the accuracy of inferred paths from prefix-level PredictRoute graphs, we randomly choose a subset of source and destination prefixes, ensuring we have not measured this path in our training data. We also ensure that the source prefixes chosen have an active RIPE Atlas probe in them. This gives us a set of paths we have not trained on but have the ability of both predicting and evaluating against a measured path.

**Prefix-level paths.** Figure 8(c) shows the edit distance between the prefix-level predicted path and the measured path for different path lengths. We note, for paths shorter than 10 prefix hops, median edit distance between PredictRoute's predicted path and the measured path is only 1.

**AS-level paths.** We now evaluate the accuracy of AS-level graphs towards a prefix. Learned in a similar manner as prefix-level DAGs, the only difference is that these DAGs are aggregated at AS-level hops. PredictRoute's AS path predictions differ from the measured path by at most 1 hop, 75% of the time (Figure 9).

**Incorporating simulation data.** A key goal of PredictRoute is to answer queries for arbitrary paths on the Internet more accurately than state of the art simulation approaches [14]. We consider two methods of incorporating simulated paths into PredictRoute. First, we consider returning the entire simulated path towards the destination prefix when there is no path from the requested source AS in the DAG. Second, we consider splicing where we return the simulated path, up until we observe an AS in the DAG. Beyond this AS, we return the path as predicted by the DAG. The idea being that with destination routing this allows us to base the latter half of the path on empirical data.

We evaluate our approach for incorporating simulated path data using ASes that are not in the DAG for a given prefix, but that contain a RIPE Atlas probe. This results in a set of 2,231 source destination pairs where we can measure the path and then compare with the predicted path.

Figure 9 shows the edit distance between measured paths and those returned by the BGP simulator (*bgpsim*) or the path produced by splicing the simulated path with the path found in the DAG (*spliced*). We observe that the PredictRoute spliced

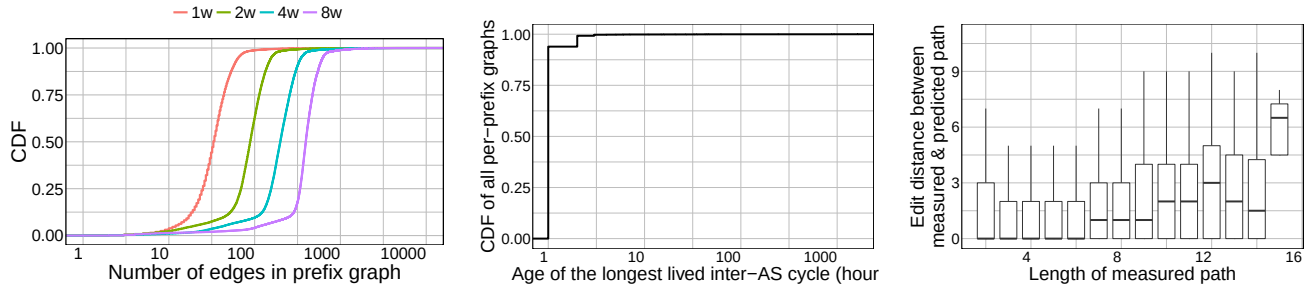


(a) Growth of destination graphs sizes with training duration.

(b) Inter-AS cyclical behavior is rare and short-lived.

(c) PredictRoute's accuracy of predicting prefix-level network paths.

Figure 8: PredictRoute prefix graph characteristics.

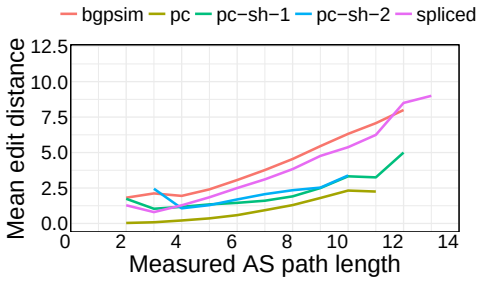


(a) Edit distance between measured and predicted paths. Lower implies higher accuracy.

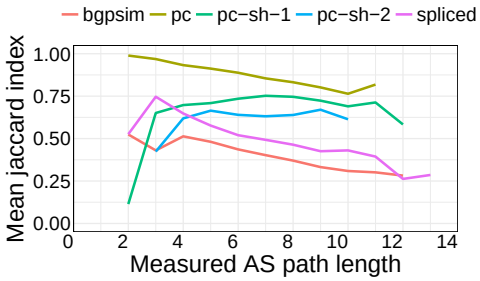


(b) Jaccard Index of measured and predicted paths. Higher implies higher accuracy.

Figure 9: Edit distance from measured paths for paths predicted directly from PredictRoute DAGs (*pc*), spliced paths with simulation (*bgpsim*) and those predicted by appending 1 (*pc-sh-1*) or 2 (*pc-sh2*) single homed stubs.

paths get at most two AS hops wrong over 82% of the time whereas simulated paths get at most two hops wrong only 50% of the time. This shows illustrates the benefits of using an approach that combines measurement and simulations even when complete measurement does not cover all paths.

**Relationship between accuracy and path probability.** We consider the probability of the highest ranked path in PredictRoute. This indicates how confident we are in our path prediction. Figure 10(a) shows the weight of the highest ranked path for paths where we predicted correctly and those where

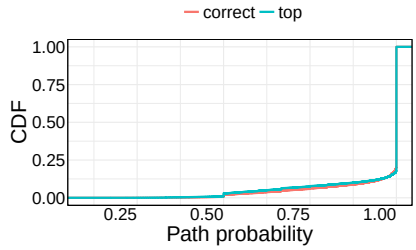


(a) Confidence of predicted paths. Over 80% of the paths have a confidence value of 1.0.

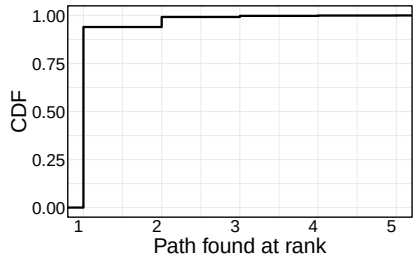


(b) 90% of accurate paths predicted by PredictRoute were the most likely (ranked 1).

Figure 10: Considering (a) the confidence value of the top ranked path and (b) the rank at which the correct path is discovered.

we did not. We see that the predicted path has a confidence of 1.0 in for nearly 80% of the paths.

We next consider how often expanding the number of paths returned increases our accuracy. Figure 10(b) shows the rank at which we find the correct path in PredictRoute's predictions. Over 90% of accurate paths are found at rank 1 highlighting that the most likely paths in PredictRoute's predictions are mostly accurate.

## 6 Comparison with Existing Systems

In this section, we compare the performance of PredictRoute with iPlane [20] and Sibyl [18], canonical works in this area.

We evaluate the three systems based on their accuracy (*i.e.,* how close is the returned path to the actual path) and their coverage (*i.e.,* for what fraction of queries can the system provide an answer).

## 6.1 Comparison Methodology

Similar to PredictRoute, iPlane consumes traceroutes and related metadata to build an *atlas* of paths. Using the atlas, iPlane predicts PoP-level paths by splicing paths in the atlas. A key piece of data consumed by iPlane is the IP-to-PoP level mapping, built from traceroutes and active measurements (*e.g.,* DNS queries) towards intermediate traceroute hops. iPlane's spliced paths serve as inputs for Sibyl [18] which then augments these predictions with confidence scores using a supervised learning algorithm [25].

To compare the accuracy of PredictRoute's path prediction with iPlane, we train PredictRoute's DAGs and iPlane's atlas on the same set of traceroutes. We extract features from iPlane's predictions to train Sibyl's supervised learning model. We use the predictions of the model (confidence scores) to evaluate Sibyl's prediction accuracy using paths with highest confidence values.

When comparing to Sibyl and iPlane, we faced the challenge that the IP-to-PoP implementation required by these systems was not available to run on new data. Thus, we acquired the set of roughly 20 million traceroutes which were used in 2016 to evaluate Sibyl (which uses iPlane's IP-to-PoP mapping). These traceroutes were performed from a wide range of vantage points: PlanetLab, RIPE Atlas and traceroute servers and looking glasses. To isolate the effectiveness of path prediction in these systems, we use the same set of 20 million traceroutes to train and test each system.

We performed five-fold cross-validation by randomly dividing the set of traceroutes into 5 groups (each with 20% of overall traces) and training the path prediction systems (iPlane, Sibyl and PredictRoute) on 4 of the 5 groups (80% of the data). We evaluate the performance of the systems on the remaining 20% of paths. We repeat this process such that each of the five folds is used for testing once. In each round, the systems were trained on 16 million and tested on 4 million traceroutes. Implementation details about the evaluation are covered in Appendix B.2.

## 6.2 Comparing accuracy of path prediction

Using the 5-fold cross validation methodology, we compare the accuracy of iPlane, Sibyl, and PredictRoute. For a given traceroute in the test data, we query each of the 3 systems and compare the predicted paths with the measured path in the test set. Since PredictRoute gives a list of path predictions ranked by their likelihood, we compare its accuracy on the highest ranked path *pc-1* and its accuracy when the second highest ranked path is included as an option *pc-2*. Similarly, Sibyl provides confidence values ($0 < c < 1$, predicted by RuleFit) for predicted paths. We consider accuracy of the top 2 paths (*sibyl-1*, *sibyl-2*) predicted by Sibyl.

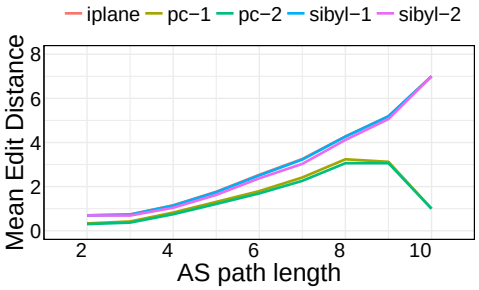


(a) Edit distance between measured and predicted paths (lower implies higher accuracy).

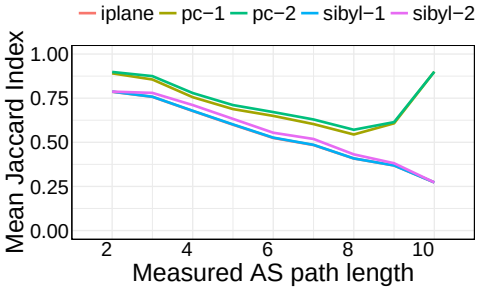


(b) Jaccard Index of measured and predicted paths (higher implies high accuracy).

Figure 11: Comparison of accuracy of PredictRoute, iPlane, and Sibyl. We find that Sibyl's weighting of returned paths improves accuracy over iPlane, but PredictRoute in general provides paths that are more similar to those observed via measurements.

We evaluate both systems' accuracy based on two distance metrics and compare these metrics relative to the length of the path being predicted.

**1. Levenshtein distance (edit distance):** This metric measures the minimum number of single-element edits (insertions, deletions or substitutions) required to change one sequence of ASes into the other. This metric takes into account the ordering of ASes on the paths being compared. In Figure 11(a), we see that PredictRoute performs better than iPlane and Sibyl for all path lengths in terms of mean edit distance. We note that as the gap in the accuracy between PredictRoute and other systems increases as the AS path length increases. However, we note that the number of paths with a length of $\geq 5$ is small, with only 10% of 2 million paths having length $\geq 5$ ASes.

**2. Jaccard Index:** This metric evaluates closeness to the measured path if order of ASes on the path is not important (*i.e.,* does the predicted path at least contain ASes from the measured path). Figure 11(b) shows the distribution of Jaccard indices of predicted and measured paths for PredictRoute, Sibyl and iPlane. Similar to edit distance, we observe Predic-

tRoute performing better than iPlane or Sibyl, in terms of Jaccard similarity of the predicted and measured paths.

We attribute PredictRoute's increased accuracy to the way that iPlane combines network paths in its path prediction. To predict a path towards prefix $P$, the initial path segment used by iPlane (from source node to intermediate hop) can be derived from any traceroute, not necessarily one that is destined to prefix $P$. Since routing is normally destination-based, this means that the first part of the path may not match the route the source would take to $P$. PredictRoute avoids this issue by predicting paths using the DAG for $P$ which is derived from traces destined towards $P$ only.

### 6.3 Comparing coverage of path queries

We now evaluate the fraction of path queries that PredictRoute and iPlane are able to respond to, given the same training dataset. We find that in each fold of the cross-validation, we query the systems for ≈2 million paths that they have not been trained on. iPlane provides paths for 70% of the queries. PredictRoute responded to 100% of the path queries. The reason that PredictRoute's is always able to predict a path is its ability to use simulated paths to fill in path segments that have not been directly observed. We discuss details of how we incorporate simulated path segments into our path predictions in §5.2. Since Sibyl leverages iPlane's predictions, it has the same coverage as iPlane.

## 7 Case Studies

In this section we demonstrate the impact of PredictRoute on real-world applications.

**PredictRoute for Refraction Networking (RN).** Refraction networking [30] is a recent technique for Internet censorship circumvention that incorporates the circumvention infrastructure into routers on the Internet. This technique has been considered more resilient to blocking by censors since it is hard to block individual routers on the Internet, while blocking source and destination of packets is relatively easy.

A key problem faced by Refraction Routing deployments today [10] is to place refraction routers in large ISPs such that client traffic gets intercepted by them. If client traffic follows a path without the refraction router on it, it leads to the failure of the refraction routing session.

We worked with the largest ISP-scale deployment of refraction routing [10] to use PredictRoute for predicting if a client refraction routing session will be successful. To predict a successful refraction routing connection, we use PredictRoute to predict the path between the client and refraction router. If the PredictRoute predicted path crosses specific prefixes within the deploying ISP, we conclude that the connection went via a refraction router and was successful (except for other non-networking failures). We find that in the current deployment of clients, PredictRoute can predict the prefix hop inside the deploying ISP which client traffic took when a RN session was successful, 100% of the time. In future, we are working towards incorporating the PredictRoute API into RN software for improved client performance.

**PredictRoute to defend against routing adversaries.** Researchers have found that anonymous communication via Tor [8] is susceptible to network-level adversaries launching routing attacks [27]. Several defenses against such attacks have been proposed that aim to avoid Tier-1 providers [5], use simulated BGP paths to avoid network-level adversaries [26], etc. PredictRoute's AS-level path prediction is highly accurate and readily available as a REST API which can be incorporated into Tor client software for defending against network-level adversaries.

## 8 Discussion and Future Work

In addition to their utility for path prediction, PredictRoute prefix graphs capture routing behavior in a novel way. We believe they can be used to revisit several classical problems in inter-domain routing. For instance:

**BGP atoms.** The networking research community has long studied the right granularity for modeling routing behavior on the Internet. One proposal is to find a set of routers that route towards the Internet similarly, called BGP atoms [2]. We note that since PredictRoute has a view of the routing behavior of all prefixes on the Internet, using measures of graph similarity across prefixes, PredictRoute's Markov chains can potentially provide a way to infer BGP atoms.

**Analyzing routing convergence.** In Section 5.1 we described the existence of cycles in PredictRoute's per-destination graphs. While these cycles are rare across ASes and have very short duration, we think they offer a new perspective on the analysis of BGP route convergence. Figure 12 shows one such cycle observed in the PredictRoute graph for prefix 122.10.0.0/19 which lasted for 3 hours. Combining PredictRoute's data plane analysis with BGP announcements can help us identify the cause of these cycles and how long it took for them to be resolved in the control as well as the data plane.

## 9 Related work

In this section, we overview related efforts for path prediction using simulations or measurements.

**Simulations for path prediction.** A number of studies rely on modeling and simulation of interdomain paths. These studies tend to model the AS-level Internet topology as a graph $G = (V, E)$ where the vertices represent ASes and the edges represent connections between them. Edges are annotated with relationships between the ASes (*e.g.,* customer-provider,

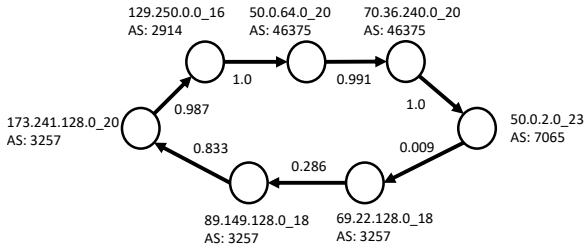


Figure 12: A cycle observed in the PredictRoute routing model of prefix 122.10.0.0/19. This cycle is across 4 ASes and lasted for 3 hours, as measured by traceroutes. Node ASNs, prefixes and edge probabilities are annotated.

peer-peer). Using this graph abstraction and a model of routing policies (*e.g.,* the Gao-Rexford model [11]), researchers can compute paths on empirical network topologies (*e.g.,* CAIDA topology [6]).

Simulations of network paths face scaling challenges due to the size of the network graph ($|V| \approx 50K$, $|E| \approx 140K$) and the fact that routing on the Internet does not follow shortest paths. Approaches to scale simulations include custom simulators [16, 28], methods to scale down the topology [19], and specialized algorithms to enable computation of policy compliant paths on the entire Internet graph [14].

In this study, we focus on algorithmic simulations [14] which enable efficient path computation on the entire AS graph. Their accuracy and limitations have been investigated by a study which finds that 65% of measured paths match those returned by the simulator [3].

**Measurement-based path prediction.** Systems like iPlane [20] predict the path from source $S$ to destination $D$ by combining paths from $S$ to an arbitrary destination with a path from an arbitrary source to $D$. This technique, referred to as *path splicing* is used to provide predictions of PoP-level paths. Note that the first part of the spliced path may be inaccurate since this portion of the path is from $S$ towards an arbitrary destination, as opposed to $D$.

In subsequent years, researchers have built iPlane Nano [21] which attempts to reduce the memory footprint of iPlane to make the usage of such a system possible on personal computers and mobiles. Unlike iPlane which stored an atlas of paths, iNano stores a graph of connectivity information (links between PoPs, ASes) observed from in traceroutes. To predict paths, iNano performs a shortest path search on the graph and predicts only those AS-level paths that conform to BGP policies and known constraints on paths (like valley free routing).

More recently, researchers leveraged iPlane's path prediction to build Sibyl [18] for optimally discovering measurements that satisfy complex path queries. In this work, the authors noted the low accuracy of path splicing (68%) and use machine learning to help improve accuracy when multiple spliced paths are available.

## 10 Conclusion

This paper introduces PredictRoute, a system that predicts network paths between arbitrary hosts on the Internet. We show analytically that it makes efficient use of available measurement platforms to maximize measurement inputs to its path prediction system. We empirically verify that its path predictions substantially improve upon the state of the art, both in terms of path query coverage and in accuracy of predicted paths. We also demonstrate PredictRoute's utility in improving applications for circumventing Internet censorship and revisiting classical inter-domain routing problems. We have released a working prototype of PredictRoute for use in Internet applications and other studies.

## References

[1] CAIDA's Prefix to ASN dataset. https://www.caida.org/data/routing/routeviews-prefix2as.xml.

[2] Y. Afek, O. Ben-Shalom, and A. Bremler-Barr. On the structure and application of bgp policy atoms. In *Proceedings of the 2Nd ACM SIGCOMM Workshop on Internet Measurment*, IMW '02, pages 209–214, New York, NY, USA, 2002. ACM.

[3] R. Anwar, H. Niaz, D. Choffnes, I. Cunha, P. Gill, and E. Katz-Bassett. Investigating interdomain routing policies in the wild. In *ACM IMC*, 2015.

[4] A. Asadpour and H. Nazerzadeh. Maximizing stochastic monotone submodular functions. *Management Science*, 62(8):2374–2391, 2016.

[5] A. Barton and M. Wright. Denasa: Destination-naive as-awareness in anonymous communications. *Proceedings on Privacy Enhancing Technologies*, 2016(4):356–372, 2016.

[6] CAIDA AS Relationship dataset. http://data.caida.org/datasets/as-relationships/.

[7] K. Chen, D. R. Choffnes, R. Potharaju, Y. Chen, F. E. Bustamante, D. Pei, and Y. Zhao. Where the sidewalk ends: Extending the internet as graph using traceroutes from p2p users. In *Proceedings of the 5th International Conference on Emerging Networking Experiments and Technologies*, CoNEXT '09, pages 217–228, New York, NY, USA, 2009. ACM.

[8] R. Dingledine, N. Mathewson, and P. Syverson. Tor: The second-generation onion router. Technical report, Naval Research Lab Washington DC, 2004.

[9] U. Feige. A threshold of ln n for approximating set cover. *J. ACM*, 45(4):634–652, July 1998.

[10] S. Frolov, F. Douglas, W. Scott, A. McDonald, B. VanderSloot, R. Hynes, A. Kruger, M. Kallitsis, D. G. Robinson, S. Schultze, et al. An isp-scale deployment of tapdance. In *7th {USENIX} Workshop on Free and Open Communications on the Internet ({FOCI} 17)*, 2017.

[11] L. Gao and J. Rexford. Stable Internet routing without global coordination. 2001.

[12] P. Gill, M. Arlitt, Z. Li, and A. Mahanti. The flattening internet topology: Natural evolution, unsightly barnacles or contrived collapse? In *International Conference on Passive and Active Network Measurement*, pages 1–10. Springer, 2008.

[13] P. Gill, M. Schapira, and S. Goldberg. Let the market drive deployment: A strategy for transitioning to bgp security. *SIGCOMM Comput. Commun. Rev.*, 41(4):14–25, Aug. 2011.

[14] P. Gill, M. Schapira, and S. Goldberg. Modeling on quicksand: Dealing with the scarcity of ground truth in interdomain routing data. *ACM SIGCOMM Computer Communication Review*, 42(1):40–46, 2012.

[15] P. Gill, M. Schapira, and S. Goldberg. A survey of interdomain routing policies. *In ACM Computer Communications Review (CCR).*, Jan 2014.

[16] J. Karlin, S. Forrest, and J. Rexford. Autonomous security for autonomous systems. *Computer Networks*, oct 2008.

[17] E. Katz-Bassett, H. Madhyastha, V. Adhikari, C. Scott, J. Sherry, P. van Wesep, A. Krishnamurthy, and T. Anderson. Reverse traceroute. In *USENIX Symposium on Networked Systems Design & Implementation (NSDI)*, 2010.

[18] E. Katz-Bassett, P. Marchetta, M. Calder, Y.-C. Chiu, I. Cunha, H. Madhyastha, and V. Giotsas. Sibyl: A practical internet route oracle. In *USENIX NSDI*, 2016.

[19] V. Krishnamurthy, M. Faloutsos, M. Chrobak, L. Lao, J.-H. Cui, and A. G. Percus. Sampling large Internet topologies for simulation purposes. 2007.

[20] H. V. Madhyastha, T. Isdal, M. Piatek, C. Dixon, T. Anderson, A. Krishnamurthy, and A. Venkataramani. iPlane: An Information Plane for Distributed Services. In *Proc. of Operatings System Design and Implementation*, 2006.

[21] H. V. Madhyastha, E. Katz-Bassett, T. E. Anderson, A. Krishnamurthy, and A. Venkataramani. iplane nano: Path prediction for peer-to-peer applications. In *NSDI*, volume 9, pages 137–152, 2009.

[22] W. Mühlbauer, S. Uhlig, B. Fu, M. Meulle, and O. Maennel. In search for an appropriate granularity to model routing policies. *SIGCOMM Comput. Commun. Rev.*, 37(4):145–156, Aug. 2007.

[23] R. Nithyanand, R. Singh, S. Cho, and P. Gill. Holding all the ases: Identifying and circumventing the pitfalls of as-aware tor client design. *CoRR*, abs/1605.03596, 2016.

[24] RIPE Atlas. https://atlas.ripe.net/.

[25] Rule Based Learning Ensembles. RuleBasedLearningEnsembles.

[26] O. Starov, R. Nithyanand, A. Zair, P. Gill, and M. Schapira. Measuring and mitigating as-level adversaries against tor. In *NDSS*, 2016.

[27] Y. Sun, A. Edmundson, L. Vanbever, O. Li, J. Rexford, M. Chiang, and P. Mittal. Raptor: Routing attacks on privacy in tor. In *24th USENIX Security Symposium (USENIX Security 15)*, pages 271–286, Washington, D.C., Aug. 2015. USENIX Association.

[28] M. Wojciechowski. Border gateway protocol modeling and simulation. master's thesis. 2008.

[29] E. Wustrow, S. Wolchok, I. Goldberg, and J. A. Halderman. Telex: Anticensorship in the network infrastructure. In *Proceedings of the 20th USENIX Conference on Security*, SEC'11, pages 30–30, Berkeley, CA, USA, 2011. USENIX Association.

[30] E. Wustrow, S. Wolchok, I. Goldberg, and J. A. Halderman. Telex: Anticensorship in the network infrastructure. In *Proceedings of the 20th USENIX Conference on Security*, SEC'11, pages 30–30, Berkeley, CA, USA, 2011. USENIX Association.

[31] J. Y. Yen. Finding the k shortest loopless paths in a network. *Management Science*, 17(11):712–716, 1971.

# Appendix

## A Extracting connectivity information from traceroutes

Using traceroutes to extract information about connectivity between prefixes and ASes on the Internet is a hard problem due to several practical issues. In this section we highlight the assumptions we made in processing traceroutes.

- **IP-to-Prefix and IP-to-ASN** We use the CAIDA prefix to ASN dataset [1] to map IP addresses to the longest matching prefix in the BGP routing table. Similarly, we associate prefixes with ASNs that announced them.
- **Dealing with prefix migration** Some prefixes are announced by different ASes at different points of time for several reasons. In order to keep track of the ASN announcing a prefix at time $t$, we use search the BGP announcements of that prefix closest to $t$.
- **Dealing with discontinuous traceroutes** Often traceroutes are discontinuous because some networks do not respond to ICMP packets. In our measurements, MegaFon (ASN 31133), Hurricane Electric (ASN 6939) and Level 3(ASN 3356) are the top 3 ASes to not respond to traceroute packets. However, we include discontinuous traces in the PredictRoute graphs in the hope that at a later point, new traces would connect the dangling traceroute to the rest of the graph.
- **Dealing with traceroutes with loops** We only added loop-free traceroutes to the PredictRoute graphs to ensure high accuracy of the system. As a result, the cycles formed in the graps are a result of 2 or more traceroutes.
- **Dealing with IXPs on path** IXPs are an important part of the interdomain routing ecosystem. We identify IXP prefixes using aggregated datasets from PeeringDB, PCH etc. PredictRoute uses this information to inform the user if their traffic crossed an IXP.

## B Details of the comparison with related work

### B.1 Resolving IP-to-PoP mappings.

Authors of iPlane gave us access to iPlane's code base. The piece of the codebase implementing IP-to-PoP mappings was missing. Therefore, we made use of an IP-to-PoP map provided by the iPlane authors which was built in 2016. We also scaled our evaluation back in time to early 2016 when this metadata was generated. Using a set of 20 million traceroutes used for evaluating Sibyl in 2016, we performed five-fold cross-validation. IPlane's atlas was trained on a set of paths and evaluated on a disjoint set of path queries (20% of all data).

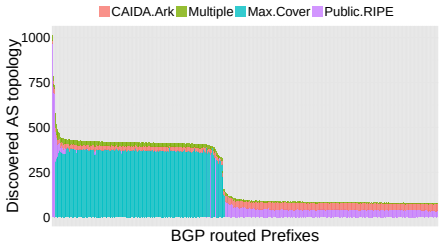


Figure 13: Number of ASes in the empirically derived directed acyclic graphs (DAGs) for each prefix. Prefixes are ranked by the number of AS included in the DAG and prefixes with less than 75 ASes in their graph are not shown, they are qualitatively similar to the ASes on the right-hand side of the graph.

### B.2 Evaluation with Sibyl

Sibyl adds a layer of ensemble based supervised machine learning on top of iPlane's predicted paths. We used the same implementation library (RuleFit [25]) as was used by the authors of Sibyl. This library is an R-wrapper around a Fortran based implementation. As a first step, we extracted features from path predictions from each fold of cross-validation. We used the same set of features used by the authors of Sibyl [18]. Since the training data in each fold, consists of 16 million traceroutes, the set of data/features used by RuleFit is correspondingly large. Nevertheless we attempted to learn a model from the training data using the same RuleFit implementation as used by Sibyl. This evaluation was done on a dedicated 252GB, 56 core server. However, the Fortran library throws memory corruption errors (SIGSEGV), when RuleFit is trained using the full 16 million traceroutes. We verified that this was not caused by our input data but was due to the large size of the input by reducing the size of the training/test datasets (using random sampling). A smaller training and test data combination leads to successful learning of the model. To resolve this issue, we randomly sampled training and test points in each fold of the evaluation, until we could get RuleFit to learn a model. The size of training data which was a threshold for this was $\approx$ 500,000 training examples. The test data had to be similarly smaller so we again randomly sampled from the 20% test queries and used the learned model to predict the confidence values of those. In this manner, we evaluate Sibyl over $\approx$ 50,000 paths overall. We reduce the testing set as well as the training set in an effort to be fair in our evaluation. We also note that we do not consider these numbers when evaluating coverage of Sibyl (which in theory should be the same as iPlane).

## C Benefits of aggregating traceroute datasets

Our atlas is comprised of per-prefix DAGs where each DAG includes ASes we have observed on paths towards the prefix. These paths may come from existing traceroute data or measurements we issue ourselves according to our greedy algorithm. Figure 13 shows the size of the DAGs for prefixes with at least 75 ASes in the DAG.

**Breadth of coverage from CAIDA Ark and RIPE Atlas Anchors.** We find that CAIDA's Ark platform is able to give us broad coverage of many destination prefixes. This follows from the fact that this platform is used to traceroute to all globally routed prefixes from a set of 25 ASes containing probes. Similarly, the public RIPE data contains broad traceroute campaigns from 200 anchor probes (higher capacity nodes that can perform more intensive measurements).

**In depth measurements of few destinations from RIPE Atlas.** The bulk of the RIPE traceroutes we ingest center on a small number of destination prefixes (*i.e.,* campaigns that traceroute from a large number of probes to a single prefix). This follows from the usage model of RIPE Atlas, which facilitates selecting many sources but not necessarily a large pool of measurement targets. Indeed, the largest DAGs we observe are for a prefix 194.0.1.0/24 announced by ASN 42909 (Community DNS) which contains 1015 ASes.

**Efficient coverage via our greedy algorithm.** Figure 13 also shows the results of running our greedy algorithm for selecting vantage points. DAGs for prefixes where we performed greedy measurements contain an average of 410 ASes (and 6886 single homed stub ASes on an average). This is in contrast to an average of 45 ASes for prefixes where we rely on existing traceroute data. We also note that this gain in terms of ASes is accomplished with a relatively small number of measurements.

## D Coverage predicted by simulations is very close to what is seen in practice.

A key question we face in using a simulator to compute coverage and select measurements to run, is whether the simulator allows us to make predictions that are close to reality. Figure 15 shows the ratio of the measured and predicted (via simulation) coverage values (*i.e.,* number of ASes covered by the DAGs). We find that in general, the simulated coverage is very close to what we observe in practice. In fact, 92.5% of the time, the predicted coverage is within 1% of the measured values.

## E Other Violations of Destination-based Routing

Not all violations of destination-based routing are based on the prior AS hop. In these cases, it is often difficult to determine exactly what rule underlies the routing behavior and we simply treat this behavior as a random process. Figure 16 shows an example where traceroutes passing through node 4 are randomly routed on the left link with probability 0.4 and routed on the right link otherwise.

This gives rise to the problem of maximizing the *expected* coverage through our choice of vantage points. The set of edges covered by each vantage point $v_i$ is now a random variable $X_{v_i}$ whose value is the edges traversed by a random walk beginning at $v_i$ and ending at $P$, where each step is chosen from the outgoing edges according to their routing probability. The problem we want to solve is:

**Problem 2** (STOC-PREFIX-COVER$_k$)**.** *Find $S \subset V'$ with $|S| \leq k$, that maximizes $\mathbb{E}[|\cup_{v\in S} X_v|]$.*

For example, in Figure 16, $X_1$ is determined by starting at 1, continuing to 3 and 4, and randomly choosing either 5 with probability 0.4 or 6 with probability 0.6. Say 5 is chosen. Then continuing to 7 and ending at $P$ yields the set of edges $X_1 = \{e_{1,3}, e_{3,4}, e_{4,5}, e_{5,7}, e_{7,P}\}$.

**Stochastic Maximum Coverage.** The above problem is special case of the *stochastic maximum coverage* problem. STOC-MAX-COVER$_k$ is a variant of MAX-COVER$_k$ where the input is an integer $k$ and $\mathcal{A} = \{A_1, A_2, \ldots\}$ where $A_i$ is a random set chosen according to some known distribution $p_i$. The goal is pick $\mathcal{A}' \subset \mathcal{A}$ to maximize $\mathbb{E}[|\cup_{A\in\mathcal{A}'} A|]$.

It can be shown that a natural extension of the greedy algorithm that, at each step, picks the set with the largest expected increase in the coverage, achieves a $1-1/e$ approximation [4]. However, note that using this algorithm in our context requires us to be *adaptive*, i.e., we select a vantage point, perform a measurement from that vantage point, and see the result of this measurement before selecting the next vantage point. This is in contrast to a *non-adaptive* algorithm that must choose the full set of $k$ vantage points before running any measurements. There is a tradeoff between these two approaches: on the one hand, an adaptive approach may provide a solution of strictly better quality than a nonadaptive algorithm since it has strictly more information.

On the other hand, the adaptive algorithm is slower since after the adaptive algorithm chooses each measurement, it must wait for the traceroute to finish before computing the next measurement. This serial computation and measurement requirement prevents parallelization. Contrast this with the nonadaptive algorithm, which can immediately generate a complete schedule of measurements without actually performing any traceroutes. This schedule can be used to perform the actual traceroutes at any time/in parallel. This flexibility makes the nonadaptive algorithm desirable in some cases despite its strictly worse solution quality. For these reasons, we implement both versions and evaluate their solution quality theoretically and experimentally. As mentioned above, the adaptive greedy algorithm is guaranteed to achieve an approximation factor of at least $1-1/e$. The non-adaptive greedy

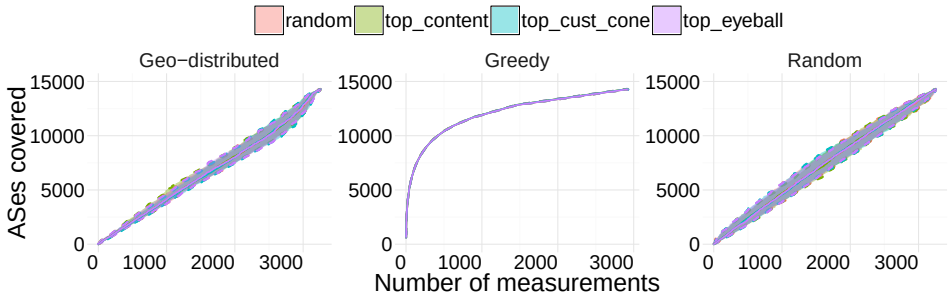


Figure 14: The number of ASes covered by the DAGs for different measurement budgets and different measurement strategies: (1) Geo-distributed (2) Greedy, and (3) Random and four destination prefix types (note that the results are consistent across prefix types).

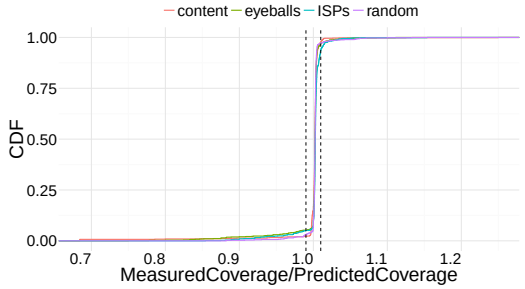


Figure 15: The measured coverage of AS graphs obtained via running traceroutes is very close to the coverage predicted by BGP policy simulations. Therefore the approximate gain of a measurement used by the greedy algorithm is close the gain obtained by running the measurement.

algorithm is guaranteed an approximation factor of at least $(1-1/e)^2$; this follows from work by Asadpour and Nazerzadeh [4] on the more general STOC-MAX-COVER$_k$ problem.

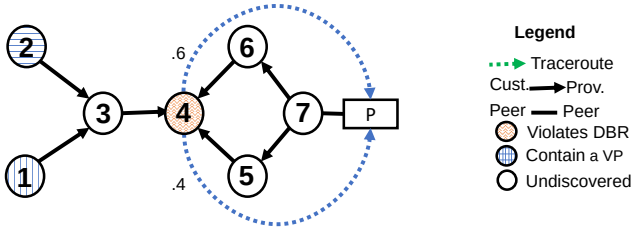


Figure 16: Traceroutes from vantage points are randomly routed from AS 4 independently among the two outgoing links according to the marked probabilities.